Journal of Microwaves, Optoelectronics and Electromagnetic Applications, Vol. 22, No. 4, December 2023
DOI: http://dx.doi.org/10.1590/2179-10742023v22i4275710

Experimental Evaluation of Through-Wall Detection Using an UWB Radar

Marcelo B. Perotoni [1], Leandro A. da Silva[1] Vinicius Silva [1]

[1] *CECS-UFABC, Santo Andre, SP, Brazil. marcelo.perotoni@ufabc.edu.br, leandro.aurelio@hotmail.com, vinifreiresilva@hotmail.com.br*

***Abstract*— This paper discusses the through-wall detection of targets behind walls using an ultra-wideband radar operating in the 2 to 15 GHz frequency range. Tests were conducted to verify its use with static and moving targets. Two real-world cases were tested: a laboratory with students sitting on benches, and an adult person standing behind a door. A fast method, based on the standard deviation, was used to transform the time-domain data matrix into a simpler waveform. This method has the potential to quickly detect the presence of human targets behind physical obstacles.**

***Index Terms*—** Tracking, through-the-wall radar, UWB radar.

I. INTRODUCTION

Technically, a signal is defined as ultra-wideband (UWB) or impulse radio when its relative bandwidth is larger than 25% [1]. UWB radars, in turn, can be practically defined as those whose bandwidhts exceed 500 MHz [2]. UWB-based radars have been used for detection of humans in several situations. For example, in post-disaster scenarios, UWB radars can be used to identify victims under rubble or collapsed trenches [3]. In defense applications [4], they can be used to check if suspicious spaces are occupied from the outside. Since its inherent non-contact nature offers easy deployment, UWB echoes can be used not only to identify whether humans are present, but also to extract biosignals. This can be done, for instance, using machine learning techniques that look for micro-Doppler signatures impressed on the UWB backscattered data [5]. Analytical methods, such as EMD (Empirical Mode Decomposition), have also been used to extract cardiac and breathing waveforms from the UWB radar return echo [6] using a 1 GHz commercial radar and an FDTD (finite difference time domain) simulation.

Using commercial UWB hardware systems, a radar based on the Novelda R2A CMOS chip transceiver coupled to a self-grounded Bow-Tie antennas (2-15 GHz range) was used to not only detect human movement, but also track the targets in real time using Kalman filtering [7]. A Salsa Ancho UWB radar, based on a Novelda XeThru X2 chipset (4.5 to 9.5 GHz), was used to implement a biomimetic sensing system [8]. A commercial UWB radar PulsON 220, covering the range from 3.15 to 5.45 GHz, was employed to detect human movement behind a drywall and wooden door by analyzing a Discrete Fourier Transform (DFT) applied to the received time-domain signal [9]. Another application involved the use of a 16-elements Vivaldi antenna array coupled to RF switches, whose signals were read by a portable vector network analyzer. The system, using the frequency range of 0.5 to 2.5 GHz, was able to visualize human targets behind a 22.5 cm concrete wall using an algorithm based on the cross correlation [10].

So far, practical through-wall detection of human presence has been achieved using waves in the ultra-high frequency (UHF) or microwave range. Cheaper techniques such as light/infrared or ultrasound are

Brazilian Microwave and Optoelectronics Society-SBMO *received 25 Jun 2023; for review 05 Jul 2023; accepted 15 Nov 2023*
Brazilian Society of Electromagnetism-SBMag *ISSN 2179-1074*

blocked by obstacles, and high-energy radiation such as X-rays are cumbersome and too costly. In terms of frequency, for through-wall applications, there is a trade-off between the material absorption, which is favored by frequencies around 1 GHz [1] and resolution, which improves for smaller wavelengths. According to [2], the optimum range for through-wall applications is between 1 and 3 GHz, which lies in a very crowded part of the electromagnetic spectrum, where mobile phone, GPS, broadcast, etc. services are allocated. Frequencies in the millimeter range benefit from much better resolution than microwaves, which enables actual imaging, but naturally incur in larger costs. Although attenuation imposed by walls and obstacles is much more intense for millimeter waves than for frequencies in the 1 GHz range, a 60-GHz off-the-shelf WiFi radio was repurposed as an imaging system, achieving success in detecting targets behind drywalls and wood panels [11]. Within the W band, centered in 93 GHz, a system based on quasi-optics achieved good results when imaging objects behind a drywall plate [12]. Millimeter-waves systems have higher costs and demand much finer mechanical precision, although recent developments for automotive radars have led to mass production of integrated circuits and systems. A comprehensive review of ultrasound, radar and through-the-wall imaging is presented in [13], and through-wall applications and their respective theory are covered elsewhere [14].

This paper discusses the use of a commercial UWB radar used for through-wall detection of humans. Section II describes the hardware and its main characteristics, including the received data format. Section III presents the clutter effects on the radar signal and compares its performance when detecting static and moving targets. Section IV presents a real-world scenario where an empty and populated classroom is illuminated by the radar. Results of this experiment are analyzed and show that the radar is effective at detecting people behind walls. Another real world experiment is presented in Section V, where a person is detected behind a wooden door.

II. RADAR HARDWARE AND ITS DATA FORMAT

The radar used in this study is the Sensorlogic Onza, which is based on the Novelda XeThru X4 integrated circuit (IC), constructed using CMOS technology [15]. The IC generates and manages the pulses in time domain, and in the reception, after amplified by a low-noise amplifier (LNA), the incoming data is converted to the digital domain by an array of comparators, operating under the swept threshold principle. The radar communicates with a host computer via a USB cable, which also provides DC power. Data traffic and logic control are performed by a BeagleBone board, which interfaces the RF and logic parts. Two linear-tapered slot antennas transmit and receive the pulses, covering the bandwidth of 5 to 11 GHz, with a maximum power of -14 dBm. The radar can detect a human target up to 10 m, according to its nominal specifications. Electromagnetic exposure and its impact on the general public is a topic of concern, a question that often arises is whether the radar poses any potential risks. In a study using the same XeThru X4 radar chipset, no statistical variation was observed in mice when subjected to a 90-day exposure [16]. The X4 System on Chip (SoC) is considered to be the first consumer UWB radar sold under USD 500 in the market, and it is compliant with the legal spectrum constraints of both Federal Communications Commission (FCC) in the US and European Telecommunications Institute (ETSI). An empirical evaluation of the repeatability of responses obtained from three X4M200 radars was presented [17], and good performance was observed for distance and angle measurements.

Data from the Onza radar can be acquired using its application programming interfaces (APIs), which can be called from within C, Python, or Matlab. In this case, a browser application was used

received 25 Jun 2023; for review 05 Jul 2023; accepted 15 Nov 2023

ISSN 2179-1074

to get the received time-domain pulses. The application connects to the hardware using its IP address. A web server running on the BeagleBone provides real-time data, with some filters available, such as Moving Target Indicator (MTI), envelope detection, and DC removal. For this specific case, data were manually saved from the web application to a comma separated value (CSV) file. Fig. 1 shows the organization of the received matrix. It is composed of real numbers, whose amplitudes are related to the time-domain received pulse voltage. The number of rows is dependent on the time duration of the data acquisition, reflecting the slow-time variable, while the fast time is represented by the columns, totaling 1536 positions. This fixed number is defined by the internal registers (ADCs) of the X4 chipset. The number of registers directly impacts in time or distance resolution.

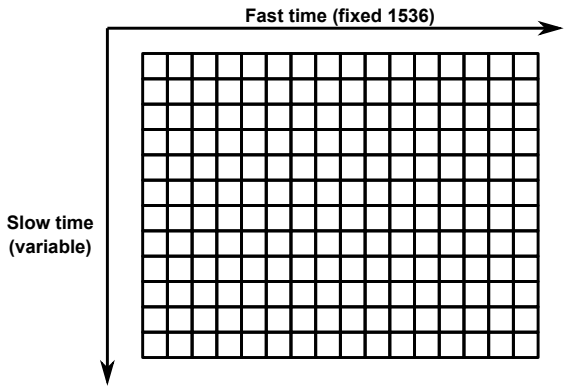

Fig. 1. Data format of the received data matrix.

In terms of timing, the fast-time sample rate is 23.3 GHz, while the slow-time sample rate is 17 Hz. This means each second of data consists of 17 consecutive readings, which can be used to capture temporal variations up to 8.5 Hz, according to the Nyquist criterion. The matrix values are purely real, due to the non-coherent reception. Each second of acquired data requires approximately 0.15 MB of storage in a .csv file.

III. Clutter and Sensitivity Measurement

To single out the contribution of the clutter, the radar must be placed in a perfect absorbing environment to minimize the backscattered energy. However, this was not available, so instead a realistic environment was tested with the radar placed on the window aperture located on the 8th floor of a building, without any frontal obstacle, according to Fig. 2(a). As shown in Fig. 2(b), a strong reflection is perceived across the initial fast-time sector (close to 5 ns), constant across the slow-time variable. This energy is due to structural reflections, from the antennas and transmission lines, and is present regardless of objects in front of the radar. Since clutter energy is always present, a simple way to eliminate it is to start visualizing the data after its energy fades out. Alternatively, successive frames (rows in this context) can be subtracted, keeping only the dynamic differences present in the signal.

To address the target measurement in the range dimension, a metallic hollow tube with 23 cm diameter and 87 cm height was placed at different positions (1, 2 and 3 meters), Fig. 3(a). Since the target was static, no differences in the received signal were observed when compared to the ambient response. This confirms the notion that this UWB radar is better suited for moving targets. To create a controlled movement, a pendulum was tested. The pendulum was a metallic cylinder (diameter 155 mm and height 335 mm) attached to a string, Fig. 3(b), swinging in front of the antennas. In addition

Brazilian Microwave and Optoelectronics Society-SBMO *received 25 Jun 2023; for review 05 Jul 2023; accepted 15 Nov 2023*
Brazilian Society of Electromagnetism-SBMag *ISSN 2179-1074*

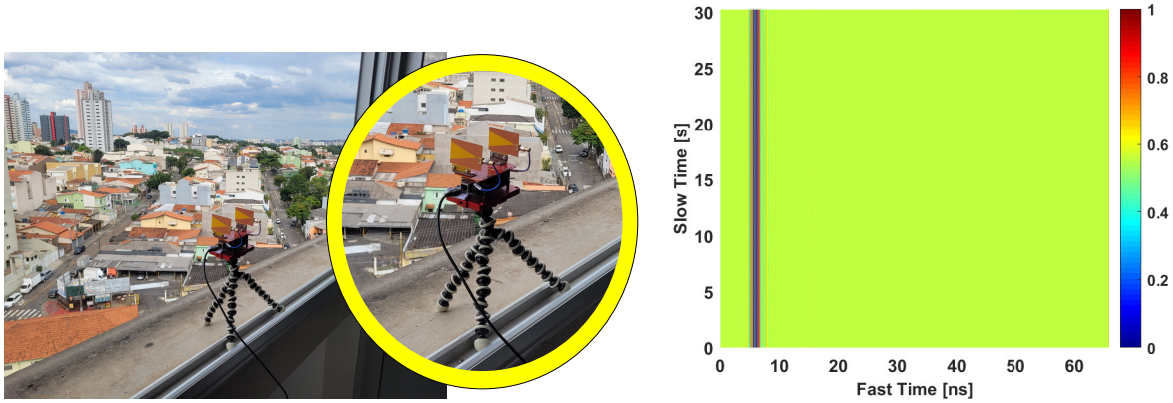

(a) (b)

Fig. 2. (a) Open view scenario, with the radar positioned on the window sill. In detail, a zoomed view of the radar and its two planar antennas (b) and its response, normalized.

to pendulums, rotating blades in fans or bicycle wheels have been used as targets for Doppler radars [18]. Two scenarios were evaluated: direct view and behind a wall Fig. 3(c). The wall was a 5-cm thick drywall used for interior divisions. In the direct view case, the pendulum was positioned 1.7 m away from the radar.The same distance was kept for the through-wall case. The UWB radar was placed approximately 15 cm away from the wall to reduce strong reflections due to antenna mismatch if it were too close to the obstacle.

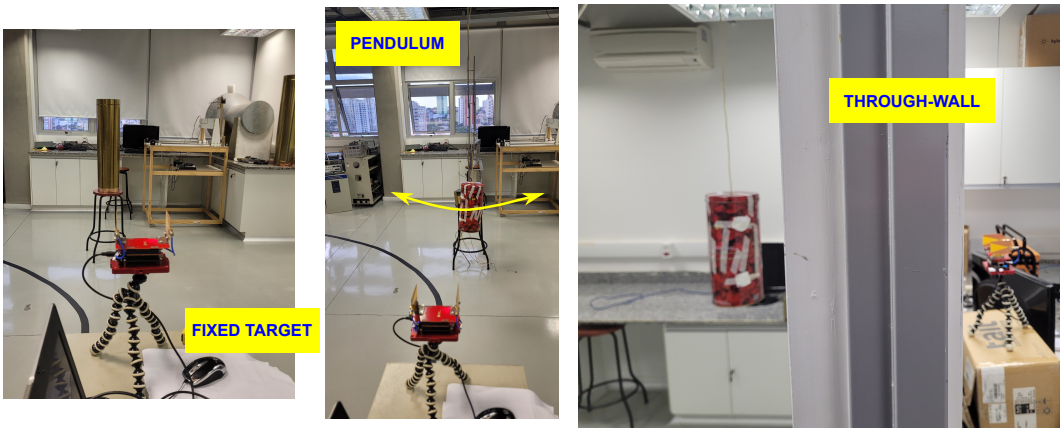

(a) (b) (c)

Fig. 3. Three scenarios for sensitivity evaluation: (a) static target; (b) pendulum in direct view and (c) same pendulum placed behind a wall. Plot is shown in log scale, after normalized.

Results for the fixed target are shown in Fig. 4. No direct indication of the target can be extracted from the plots. Further processing is needed [14], using Synthetic Aperture Radar (SAR) techniques. In SAR, the received pulse is transformed to the frequency domain, and the movements of the radar relative to the image emulates a larger antenna aperture. However, SAR techniques are more demanding in terms of processing.

For the case of the swinging pendulum, results are shown in Fig. 5. Its movement is directly seen in both cases. The only difference between the behind-the-wall, Fig. 5(b) and the direct view, Fig. 5(a) is the relative amplitude of both responses.

In terms of waveforms and their respective frequency spectra, the 20th rows from the matrices relative

ISSN 2179-1074

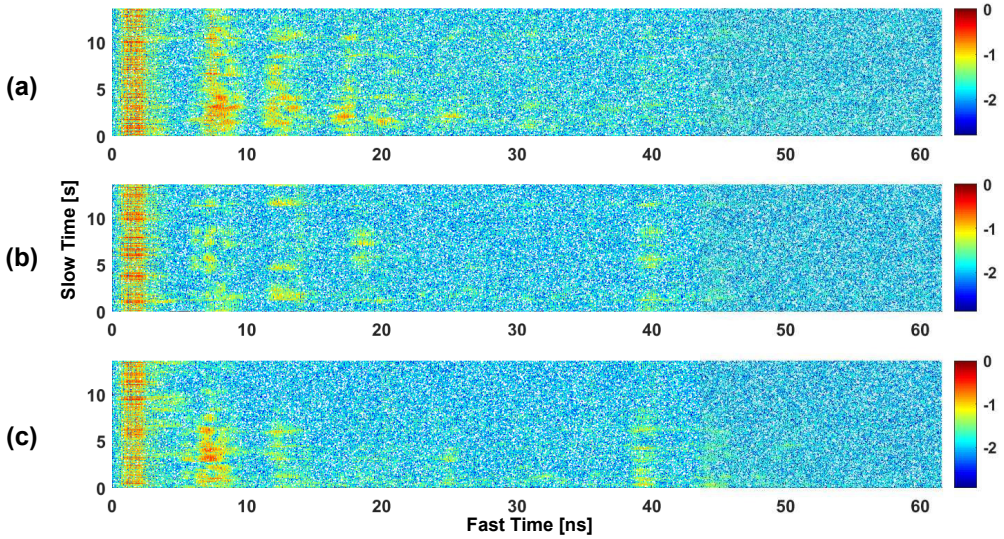

Fig. 4. Received data after the static cylinder placed in three different distances; 1 m (a), 2 m (b) and 3 m (c) . Amplitudes are shown in log scale, normalized.

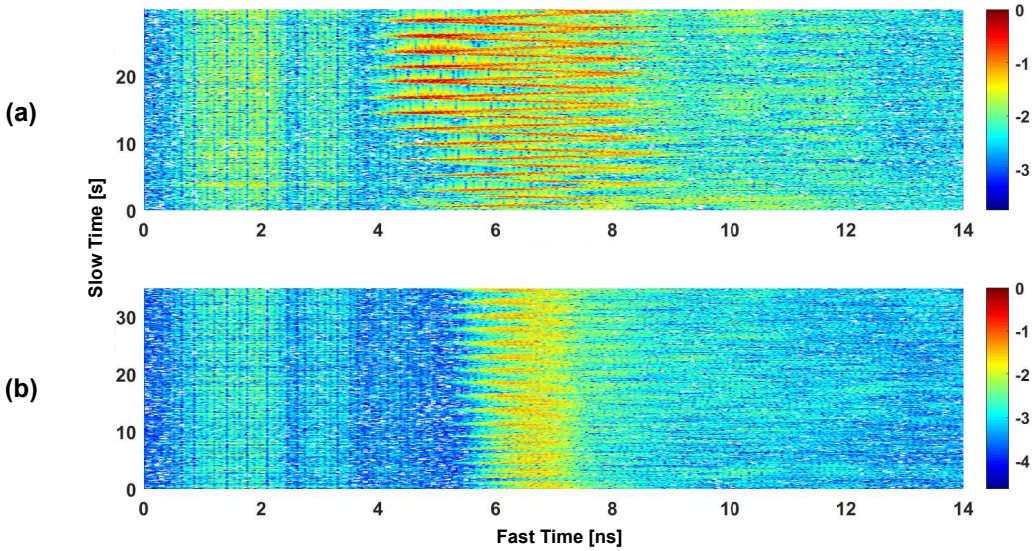

Fig. 5. Received data for the moving pendulum in direct view (a) and behind-the-wall (b).

to the scenarios open view (Figs. 2(a)) and moving pendulum (Fig. 3(b)) were individually evaluated. Fig. 6 depicts the normalized signals in both time (Fig. 6(a)) and frequency (Fig. 6(b)) domains. From the power spectra plot, it is possible to see that most of the pulse energy lies in between 6 and 8 GHz.

A relevant point to address is the comparison between a human target and the pendulum. Human body radar cross section (RCS) was measured in [19], and is compared against the pendulum simulations carried out by the Method of Moments (MoM) in FEKO, and the respective analytical formula (radius r, height h and wavelength λ) RCS [20]:

$$RCS = \frac{2\pi r h^2}{\lambda}. \tag{1}$$

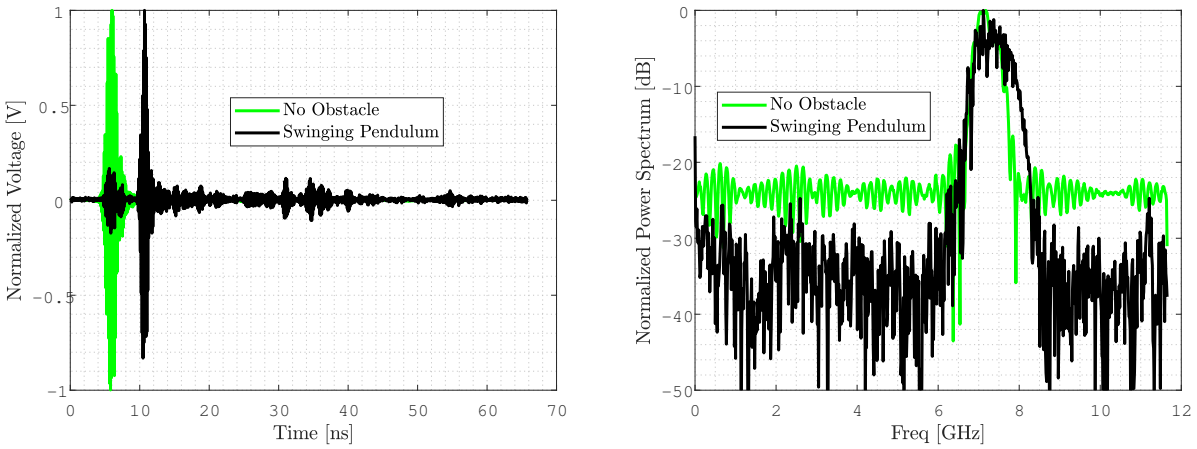

(a) (b)

Fig. 6. Signal waveforms (a) and their power spectra (b) for the a sample of the received signals of the scenario without obstacle and the pendulum used as target.

where RCS is given in square meters [m^2]. From the comparison shown in Fig. 7 one can see that the pendulum, in spite of its smaller size, has lower cross-sectional area for this specific frequency range, when compared to a human target. However, both the analytical formula and the numerical evaluation represent an upper-bound value for the RCS, where the wave polarization is parallel all the time to the cylinder axis, and no further scattering is present in the ambient. In addition to it, the noticeable increase in the human body RCS at lower frequencies (below 2 GHz) also indicates this range as better suited for through-wall detection, with the trade-off of larger antennas.

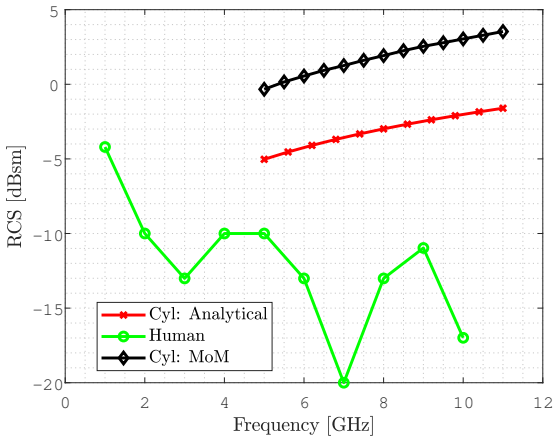

Fig. 7. RCS of a human body [19] and of the pendulum, the latter from the analytical formula and with electromagnetic simulation.

IV. Behind the Wall Real Scenario I: Classroom

A real-world scenario was conducted in a laboratory class where students performed tests at benches. About 15 people were in the space (40 m^2), with moderate movements. Fig. 8(a) shows the position where the radar was placed, about 10 cm from a drywall panel, and the populated area, Fig. 8(b). Results are shown in Fig. 9, for an empty room and also for five different periods, each with the

ISSN 2179-1074

populated space. No processing was performed on the data, so the plots reflect the raw backscattered data acquired by the receiver antenna. It is possible to see that when there is no movement behind the wall, only clutter and reflections from the environment are cause for the visible traces along the fast-time axis. Movement is visualized by the interruptions seen on the plots, where there is a break in the data homogeneity.

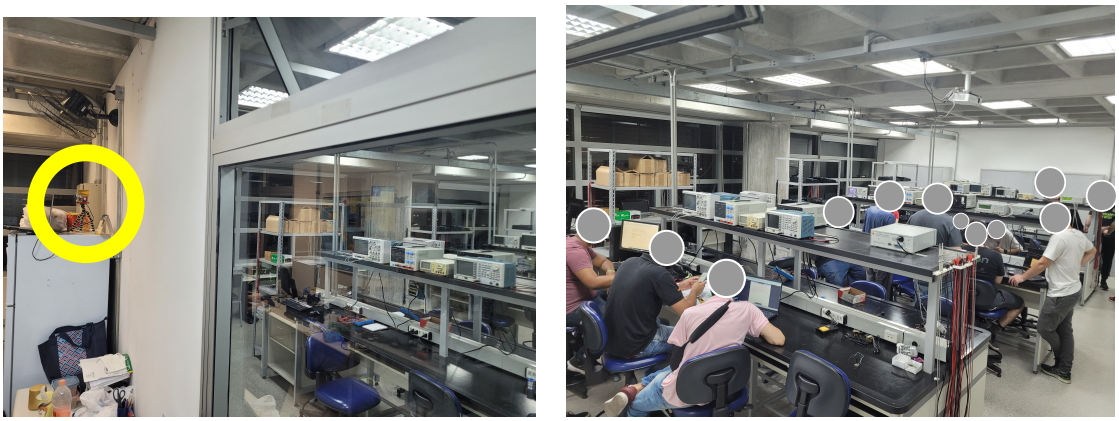

(a) **(b)**

Fig. 8. Radar positioned to view the behind-the-wall scenario, empty (a), and populated with students (b).

Automatic detection of human presence can be implemented using machine learning techniques, which compare several samples taken in a variety of scenarios [21], [22]. However, the model must be trained for different types of areas, and some of the samples need the place to be empty, which is not always possible.

A simpler mathematical procedure to identify variations across one of the dimensions of the matrix is the standard deviation. If the scattered data is given in an $m \times n$ matrix, the standard deviation σ_j of the j$^{\text{th}}$ column is given by:

$$\sigma_j = \sqrt{\frac{\sum_{i=1}^{m} (X_{ij} - \mu_j)^2}{m-1}}. \tag{2}$$

where μ_j is the median of the j$^{\text{th}}$ column. Upon applying this operation to the data shown in Fig. 9, the results are shown in Fig. 10. The information encoded in two dimensions can be reduced to a single one, where the movements seen behind the wall are translated into a larger amplitude σ. By using a threshold baseline on the standard deviation an automatic presence detector heuristic can be devised, where the direct processing of the incoming waves triggers the indication of human presence.

ISSN 2179-1074

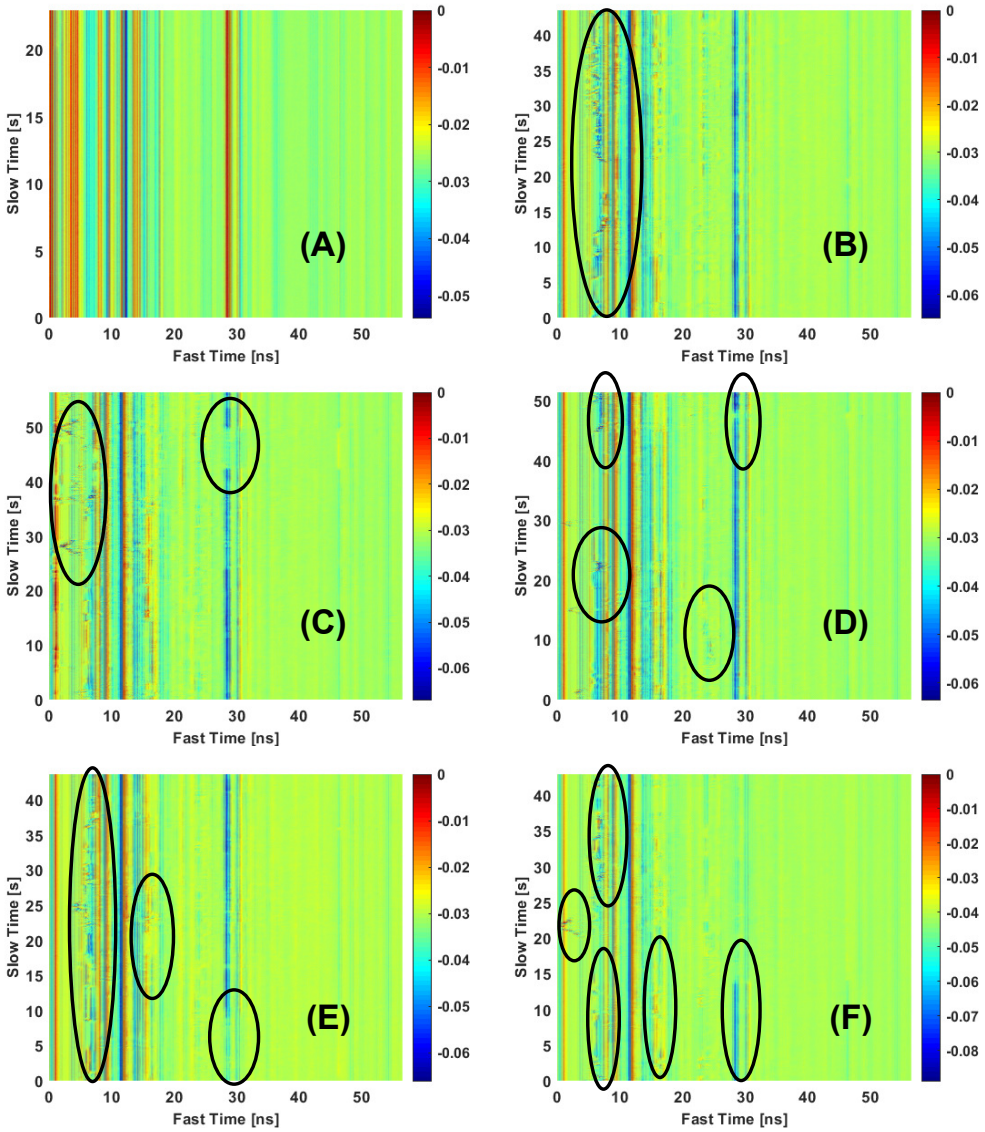

Fig. 9. Scattered signal from the class, empty (A), and different samples of the occupied laboratory (B to F). Results are stressed within black ellipses, showing indication of movement. Scale is logarithmic, normalized.

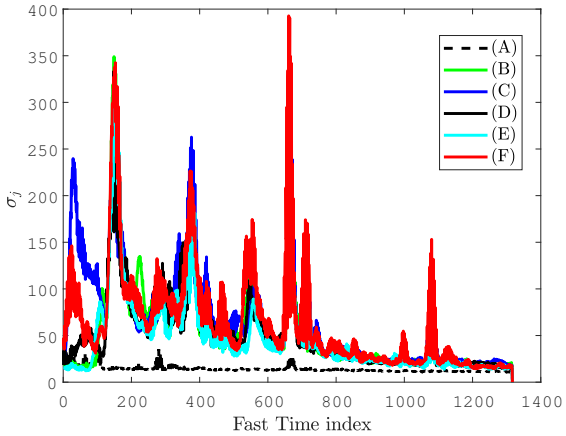

Fig. 10. Standard deviation of the plots shown in Fig. 9, applied column-wise. The broken line indicates the empty room.

V. Behind the Wall Real Scenario II: Is There Someone Behind a Door?

A second scenario was investigated whether the UWB radar was able to detect an adult standing motionless right behind a close wooden door. A modified ground penetration radar (GPR), operating at continuous wave frequency of 1.6 GHz, was used for investigating the presence of a human target through a wall [2]. In order to avoid backside radiation from the target, an antiradar coating was used. Information on the occupancy is relevant for police and security services in case of breaking into a place, to avoid using lethal force. Here, the radar was positioned 1.3 m from the ground, 20 cm from the door. The subject was an adult, trying to stay as steady as possible, shown as in Fig. 11(a) along with the raw acquired data, normalized in decibels for the two scenarios, 11(b) and 11(c). Differences are hardly noticed due to the large clutter, when both matrices shown in the plot are taken into account. If the radar is moved away from the door, in order to separate the fast-time of the clutter and the subject, its sensitivity will decrease due to the attenuation.

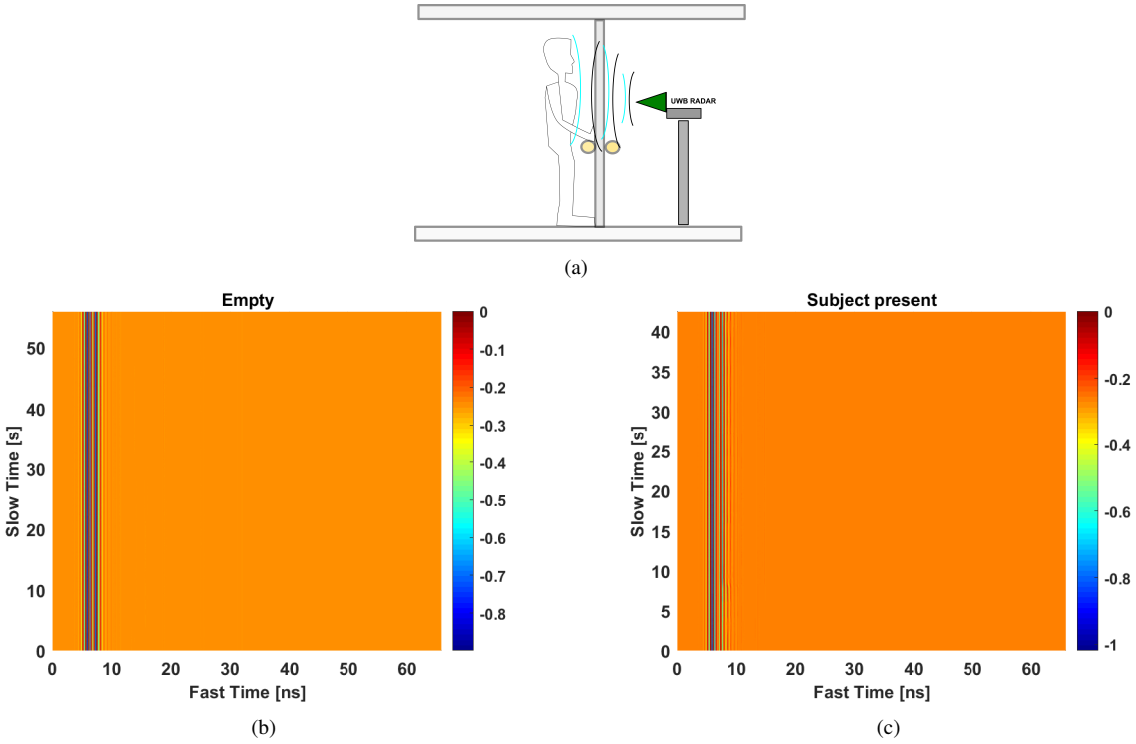

(a)

(b)

(c)

Fig. 11. Behind the door investigation diagram (a) and respective raw data for the (b) empty and when occupied (c) rooms.

In order to identify the subject presence, the same standard deviation analysis is followed, as seen in the previous section, and the respective results are shown in Fig. 12. The presence of a subject behind the door is noticeable, due to the larger amplitude seen across the fast-time variable. Small-amplitude body movements and breathing are responsible for these oscillations, within the sensibility of the Onza radar, which captures these small time variations impressed on the reflected signal. A similar study was performed using a commercial UWB radar (band of 3.15 to 5.45 GHz), using Singular Value Decomposition (SVD) and Short-time Fourier Transform (STFT) to help detect the target [23], which are more computationally demanding than the standard deviation here employed.

ISSN 2179-1074

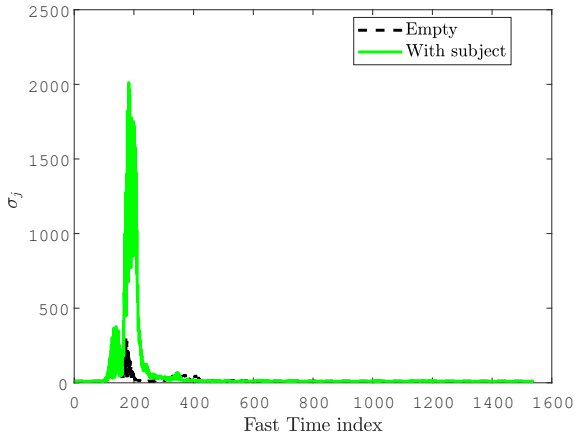

Fig. 12. Standard deviation of the plots shown in Fig. 11, applied column-wise.

VI. Conclusion

This article covered the experimental through-wall detection of humans using a commercial UWB radar. A pendulum was used as target for addressing the system overall sensitivity and its application for steady scenarios, as well as the differences imposed on the backscattered data when the same target was behind a wall. Two real-world scenarios are then analyzed in order to see if there is human activity behind a wall: a laboratory classroom populated by students and a wooden door with a person right behind it. A standard deviation technique was used in order to help identify the human presence, which is faster and effective separating clutter and noisy elements from the actual echo coming from moving targets.

Comparing the proposed system to other reports, for instance machine-learning based methods [5], [21], [22] require large training datasets, therefore not allowing a quick deployment and general scenario visualization. The standard deviation here used is also easier implemented and faster than analytical methods such as EMD [6] and SVD [23]. Its hardware is also of comparable cost and more robust than network-analyzer-based with switching antennas [10] and millimeter-wave or infrared platforms [12].

The offline operation, i.e., data had to be saved prior to the processing, was found to be the most problematic item using this approach. It does not allow real-time analysis, and results in large files. The operation can be made faster with direct access to the data on-the-fly, using Python as interface instead of a browser, for instance, and it is currently under investigation.

Acknowledgment

This project was supported by Sao Paulo Research Foundation (FAPESP), grant #2019/12268-4 (PIPE Program).

References

[1] S. Nag, M. A. Barnes, T. Payment, and G. W. Holladay, "An ultra-wideband through-wall radar for detecting the motion of people in real time," *Proc. SPIE*, vol. 4744, pp. 48 – 57, 2002.

[2] J. D. Taylor, *Advanced Ultrawideband Radar: signals, targets and applications*. CRC, Boca Raton, 2017.

[3] L. Zhao, M. Yangyang, Z. Yang, L. Fulai, Y. Xiao, Q. Fugui, L. Hao, L. Guohua, and W. Jianqi, "UWB radar features for distinguishing humans from animals in an actual post-disaster trapped scenario," *IEEE Access*, vol. 9, pp. 154 347–154 354, 2021.

  ISSN 2179-1074

[4] P. Withington, H. Fluhler, and S. Nag, "Enhancing homeland security with advanced UWB sensors," *IEEE Microwave Magazine*, vol. 4, pp. 51–58, 2003.

[5] F. Qi, F. Liang, M. Liu, H. Lv, P. Wang, H. Xue, and J. Wang, "Through-wall detection and classification of human activities using uwb bio-radar," *IEEE Antennas and Wireless Propagation Letters*, vol. 18, pp. 437–441, 2019.

[6] L. Liu, Z. Liu, and B. E. Barrowes, "Through-wall bio-radiolocation with UWB impulse radar: Observation, simulation and signal extraction," *IEEE Journal of Selected Topics in Applied Earth Observations and Remote Sensing*, vol. 2011, pp. 791 – 798, 2011.

[7] Y. Yu, T. McKelvey, and B. Stoew, "A compact UWB indoor and through-wall radar with precise ranging and tracking," *International Journal of Antennas and Propagation*, vol. 2012, pp. 1–11, 2012.

[8] G. Schouten and J. Steckel, "RadarSLAM: Biomimetic SLAM using ultra-wideband pulse-echo radar," in *2017 International Conference on Indoor Positioning and Indoor Navigation (IPIN)*, pp. 1 – 8, 2017.

[9] S. D. Liang, "Sense-through-wall human detection based on UWB radar sensors," *Signal Processing*, vol. 126, pp. 117 – 124, 2016.

[10] Z. Hu, Z. Zeng, K. Wang, W. Feng, J. Zhang, Q. Lu, and X. Kang, "Design and analysis of a UWB MIMO radar system with miniaturized vivaldi antenna for through-wall imaging," *Remote Sensing*, vol. 2019, pp. 1 – 20, 2011.

[11] F. Zhang, C. Wu, B. Wang, and K. J. R. Liu, "mmeye: Super-resolution millimeter wave imaging," *IEEE Internet of Things Journal*, vol. 8, pp. 6995–7008, 2021.

[12] U. Alkus, A. B. Sahin, and H. Altan, "Stand-off through-the-wall w-band millimeter-wave imaging using compressive sensing," *IEEE Geoscience and Remote Sensing Letters*, vol. 15, pp. 1025–1029, 2018.

[13] C. Clemente, A. Balleri, K. Woodbridge, and J. Soraghan, "Developments in target micro-doppler signatures analysis: radar imaging, ultrasound and through-the-wall radar," *EURASIP Journal of Advances in Signal Processing*, vol. 47, pp. 1–18, 2013.

[14] M. G. Amin, *Through-the-wall Radar Imaging*. CRC, Boca Raton, 2011.

[15] *X4 Datasheet*, Novelda AS, 2 2023, rev. A.

[16] Y. Zhang, X. Guo, T. Li, M. Zhang, Y. Feng, W. Li, X. Zhu, R. Gu, and L. Zhou, "Effect and safety evaluation of xethru x4 radar radiation on sexual hormone levels in mice," in *2019 41st Annual International Conference of the IEEE Engineering in Medicine and Biology Society (EMBC)*, pp. 1318–1320, 2019.

[17] F. Thullier, A. Beaulieu, J. Maitre, S. Gaboury, and K. Bouchard, "A systematic evaluation of the xethru x4 ultra-wideband radar behavior," in *11th International Conference on Current and Future Trends of Information and Communication Technology in Healthcare ICTH 2021*, pp. 148–1555, 2021.

[18] H. C. Kumawat and A. B. Raj, "Extraction of doppler signature of micro-tomacro rotations/motions using continuous wave radar-assisted measurement system," *IET Science, Measurement and Technology*, vol. 14, pp. 772–785, 2020.

[19] E. Piuzzi, P. D'Atanazio, S. Pisa, E. Pitella, and A. Zambotti, "Complex radar cross section measurements of the human body for breath-activity monitoring applications," *IEEE Transactions of Instrumentation and Measurement*, vol. 64, pp. 2247–2258, 2015.

[20] T. Maamria and H. Kimouche, "Investigation of monostatic rcs measurement for simple and complex shapes at 9.4 GHz," in *2015 Fourth International Conference on Electrical Engineering (ICEE)*, pp. 1 – 5, 2015.

[21] X. Li, Y. He, and X. Jing, "A survey of deep learning-based human activity recognition in radar," *Remote sensing*, vol. 11, pp. 1–22, 2019.

[22] J. A. B. et al., *Methods and Techniques in Deep Learning*. IEEE Press, 2023.

[23] S. Singh, Q. Liang, and L. Sheng, "Sense through wall human detection using UWB radar," *EURASIP Journal of Wireless Communications and Networking*, vol. 20, pp. 1 – 11, 2011.

received 25 Jun 2023; for review 05 Jul 2023; accepted 15 Nov 2023

ISSN 2179-1074